RAIRS and TPD Study of Methyl Formate, Ethyl Formate, and Methyl Acetate on Ni(111)

E. Zahidi, M. Castonguay, and P. McBreen*

Contribution from the Département de chimie, Université Laval, Québec, G1K 7P4, Canada

Received August 29, 1993®

Abstract: The thermal chemistry of methyl formate, ethyl formate, and methyl acetate on Ni(111) was studied using infrared reflection absorption spectroscopy and temperature programmed desorption. The principal molecular decomposition products in each case were CO and H_2. Methane and acetaldehyde were also formed from ethyl formate. For each of the three molecules, adsorption occurred through the interaction of the carbonyl lone pair with the metal. The orientation of the molecular plane, in each case, was approximately perpendicular to the surface. The molecular surface decomposition species were detected by RAIRS. Methoxy species were formed from methyl formate and methyl acetate. Ethoxy was produced by ethyl formate. Evidence was obtained for the formation of a stable acetyl species during the decomposition of methyl acetate. The decomposition of methyl acetate occurred above 170 K whereas the other two esters began to decompose at approximately 140 K. This study shows that the adsorption induced shifts in the infrared spectra of esters are similar to those which occur on the formation of ester–Lewis acid adducts.

Introduction

A reflectance infrared study of the three simple esters shown below provides the basis for the investigation of several interesting aspects of surface chemistry:

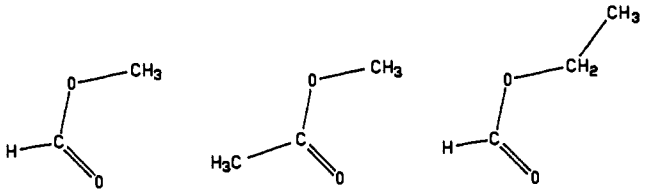

METHYL FORMATE METHYL ACETATE ETHYL FORMATE

These three molecules contain the OCO functional group and therefore present a variation on the well-studied chemisorption of formic acid on metals. The different substituent groups will have an influence on the role of steric effects in the packing of the adsorbates on the surface. The substituent groups should also play a role in determining the surface reactivity of these molecules. In terms of reaction selectivity, esters are interesting because surface decomposition could occur through cleavage of the C_1–O_e bond (where C_1 is the carbonyl carbon and O_e is the ester oxygen) to form CO and alkoxy species or alternatively cleavage of the O_e–alkyl bond to form adsorbed formate and alkyl species. In both cases, the decomposition process transforms a low-symmetry species into a high-symmetry species and hence both should be particularly amenable to study using reflectance IR. An important aspect of the surface chemistry of these esters is that they are weakly bound species.[1,2] As a result, their heats of adsorption are close to both the activation energies for surface decomposition and the cis–trans isomerization energies.[3] This means that desorption will be competitive with reaction, and that the reaction probability may sensitively depend on the nature of the substituent groups. It also means that isomerization may occur on adsorption, particularly at high coverages where steric repulsion will be greatest.

The adsorption of methyl formate has been studied on Ag(110) by Barteau *et al.*,[4] W(100) by Worley and Yates,[5] and Cu(110) by Sexton *et al.*[1,2] The latter authors reported molecular desorption of methyl formate from clean copper, with a heat of desorption of ~40 kJ mol^{-1}. Pre-exposure of the copper surface to oxygen induced a reaction leading to adsorbed formate and methoxy, as determined by HREELS measurements. Their HREELS measurements also indicated that methyl formate chemisorbed on the clean surface via the carbonyl oxygen, with the molecular plane perpendicular to the surface.

Methyl formate is an interesting and frequently studied species in metal-based heterogeneous catalysis.[1,2,6-14] The Tischenko reaction, in which the dimerization of formaldehyde yields methyl formate, is catalyzed by unsupported copper. As discussed in more detail by Sexton *et al.*,[1,2] methyl formate may also be synthesized over copper-based catalysts via the dehydrogenation or condensation of methanol, or by the catalytic reaction of formaldehyde with methanol.[14] Conversely, the hydrogenolysis of methyl formate yields methanol, and methyl formate is often a byproduct in the synthesis of methanol.[7] Methyl formate can also be produced by the carbonylation of methanol, and subsequent hydrogenolysis produces two methanol molecules. The latter sequence of reactions is a possible method for low-temperature methanol synthesis.[6] The reactivity of weakly bound species such as methanol and methyl formate is hard to study in UHV, since the desorption energy (E_d) may be less than or equal to the activation energy for reaction. Nevertheless, the coverage of weakly bound species may be significant under the high-pressure conditions typical of industrial catalysis, and such species may

* Abstract published in *Advance ACS Abstracts*, May 1, 1994.

(1) Sexton, B. A.; Hughes, A. E.; Avery, N. R. *Appl. Surf. Sci.* **1985**, *22/23*, 404.
(2) Sexton, B. A.; Hughes, A. E.; Avery, N. R. *Surf. Sci.* **1985**, *155*, 366.
(3) Wiberg, K. B.; Laidig, K. E. *J. Am. Chem. Soc* **1987**, *109*, 5936.
(4) Barteau, M. A.; Bowker, M.; Madix, R. J. *Surf. Sci.* **1980**, *94*, 303.
(5) Worley, S. D.; Yates, J. T., Jr. *J. Catal.* **1977**, *48*, 395.
(6) Gormley, R. J.; Rao, V. U. S.; Soong, Y.; Micheli, E. *Appl. Catal. A* **1992**, *87*, 81.
(7) Millar, G. J.; Rochester, C. H.; Waugh, K. G. *J. Chem. Soc., Faraday Trans.* **1991**, *87*, 2785.
(8) Fakley, M. F.; Jennings, J. R.; Spencer, M. S. *J. Catal.*, **1989**, *118*, 483.
(9) Broun Bourzutschky, J. A.; Homs, N.; Bell, A. T. *J. Catal.* **1990**, *124*, 73.
(10) Lee, J. S.; Kim, J. C.; Kim, Y. G. *Appl. Catal.* **1990**, *57*, 1.
(11) Monti, D. M.; Cant, N. W.; Trimm, D. L.; Wainwright, M. S. *J. Catal.* **1986**, *100*, 17.
(12) Monti, D. M.; Cant, N. W.; Trimm, D. L.; Wainwright, M. S. *J. Catal.* **1986**, *100*, 28.
(13) Cant, N. W.; Tonner, S. P.; Trimm, D. L.; Wainwright, M. S. *J. Catal.* **1985**, *191*, 197.
(14) Chung, M.-J.; Moon, D.-Ju; Park, K.-Y.; Ihm, S.-K. *J. Catal.* **1992**, *136*, 609.

0002-7863/94/1516-5847$04.50/0

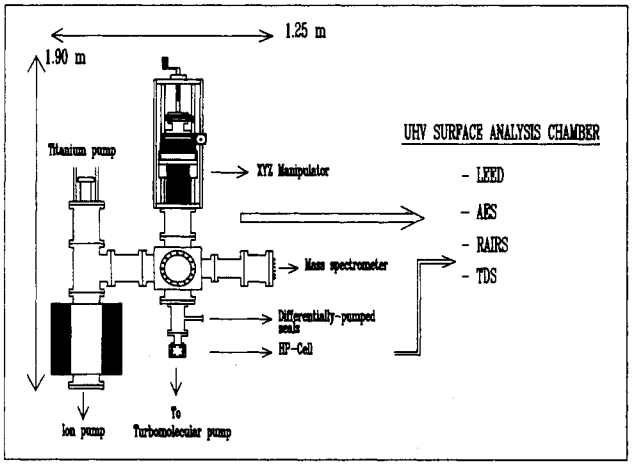

Figure 1. Schematic diagram of the UHV chamber and the high-pressure reaction cell.

play an important and active role in the catalytic cycle. The role of adsorption strengths in limiting the scope of UHV studies is discussed in more detail by Sexton and co-workers.[1,2] One way to confront this problem is to perform combined UHV–high pressure reaction cell studies. To this end, we have constructed such a system for in situ RAIRS studies over the pressure range 10^{-10} to 10^{+3} Torr. The results of studies using the latter system will be reported separately. In this paper we will concentrate on the orientation of the adsorbed ester molecules and the general details of their surface chemistry on Ni(111). Nickel is chosen as a substrate since the typically stronger interaction of adsorbates with nickel, as compared to copper, should allow us to probe a wider range of ester surface chemistry under UHV conditions.

Experimental Section

The experiments were performed using the upper part of the two level UHV–high pressure reaction cell system illustrated in Figure 1. The Ni(111) sample, purchased from Monocrystals Inc., was cleaned by repeated cycles of sputtering, oxygen treatment, and annealing to 900 K. Surface cleanliness was verified using retarding field Auger, CO desorption, and RAIRS measurements on adsorbed CO. The adsorbate liquids were purified by repeated freeze–thaw cycles.

The infrared spectra were collected using a Mattson Galaxy 4020 FTIR spectrometer with a 1 mm^2 active area narrow band MCT detector. The IR path was set up as follows: the unpolarized, collimated beam exits the spectrometer via the external port, passes through a polarizer, is deflected 90° upward to the UHV level by a flat mirror, and then is focused on the sample by a 250 mm effective focal length parabolic mirror. The flat mirror also allows redirection of the beam 90° downward to a high-pressure cell. In the UHV chamber, the beam impinges on the crystal with an angle of incidence of 86° with respect to the surface normal. The reflected beam is recollimated by another 250-mm parabolic mirror. Final focusing on the detector is accomplished by a 75°, 50-mm parabolic mirror. The beam exits and enters the chamber through a set of differentially pumped Viton O-ring sealed NaCl windows. The MCT detector sets the experimental low frequency cutoff at around 750 cm. However, the signal-to-noise ratio below 920 cm^{-1} was not satisfactory in our data. A 42-kHz low-pass filter is used for removing the higher frequency signal in the double-sided interferograms to avoid folding-in of the noise from outside the spectral region.

The reported spectra are expressed in absorbance units and represent the ratio of 1000 sample scans to 1000 background scans. Spectra were recorded with a 4-cm^{-1} optical resolution in only one direction of the moving mirror. The mirror speed was 6.33 cm/s for an acquisition time of 2.56 min. Digital processing of the spectral data consists of 4× zero-filling, yielding a digital resolution of 1.0 cm^{-1} and triangle apodization.

Results

1. Temperature-Programmed Desorption Results. The TPD spectra for methyl formate (MF), ethyl formate (EF), and methyl acetate (MA), shown in Figures 2–4, respectively, display several features in common. A low-temperature peak indicative of multilayer desorption appears at 120, 128, and 136 K for MF, EF, and MA, respectively. Desorption from the monolayer occurs

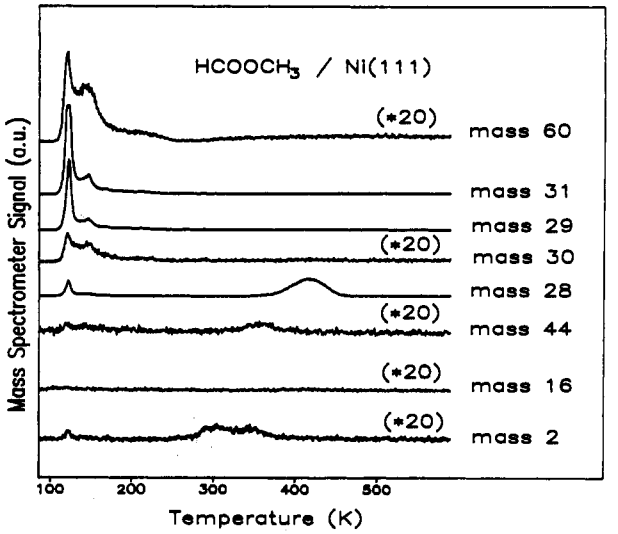

Figure 2. TPD spectra obtained following approximately 10 L exposure of Ni(111) at 86 K to methyl formate. Heating rate, 0.5 K/s.

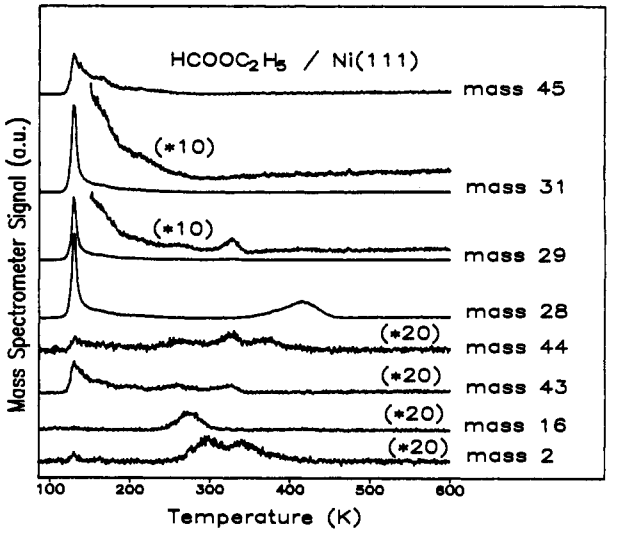

Figure 3. TPD spectra obtained following approximately 10 L exposure of Ni(111) at 86 K to ethyl formate.

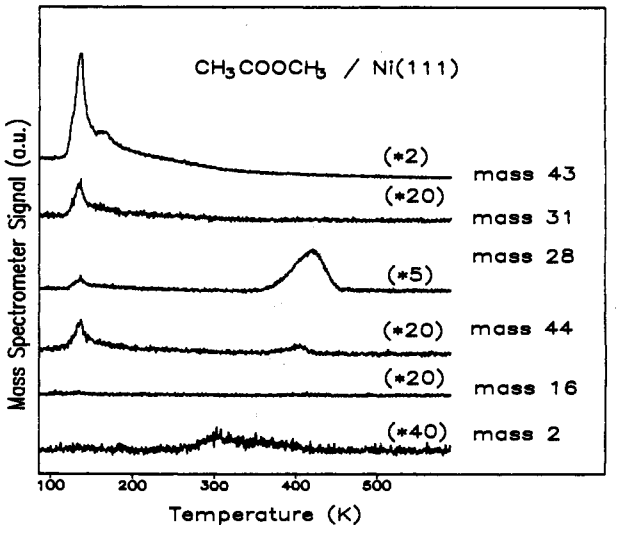

Figure 4. TPD spectra obtained following approximately 7 L exposure of Ni(111) at 86 K to methyl acetate.

in a broad peak at 142, 136, and 165 K for MF, EF, and MA, respectively. It should be noted that the spectra in Figures 2–4 are in fact each composites of two different experiments. In each experiment four masses were selected. The exposure conditions, that is the position of sample with respect to the doser, may have been different in each experiment. The consequent difference in coverage from experiment to experiment accounts for the differences in the ratio of multilayer-to-monolayer signal which appear in each of the three TPD figures. The TPD traces displayed in Figures 2–4 evidently result from greater than monolayer coverages and are not entirely characteristic of molecular desorption from submonolayers. The fairly complex coverage dependence of the desorption spectra will be presented separately in conjunction with the coverage-dependent RAIRS data.[15] The coverage dependence of the TPD traces may be summarized as follows. Dissociative adsorption of MF and EF occurs for low coverages on Ni(111). Some molecular desorption sets in, in both cases, at approximately 50% of the exposure required to begin populating the condensed layer. In the case of MF, molecular desorption intensity is distributed among peaks at 164 and 208 K. With increasing coverage the intensity of the low-temperature peak increases and its position shifts to the 142 K position shown in Figure 2. Ethyl formate displays similar behavior in that molecular desorption distributed among peaks at 170 and 223 K sets in at approximately 50% of the exposure required to form the condensed layer. On increasing the exposure, the low-temperature peak increases in intensity and a shoulder at 143 K appears prior to formation of the condensed layer. Methyl acetate displays a different behavior in that molecular desorption at 207 K is observed at low coverages. On increasing the exposure the molecular desorption peak shifts to the 165 K position shown in Figure 4. The nature of the decomposition products, however, did not change as a function of the surface coverage for any of the three molecules.

CO and H_2 are the major desorption products resulting from dissociative adsorption of MF, EF, and MA. In each case the CO desorption feature peaks at $T_{max} \approx 410$ K. Similarly, for each of the three adsorbates, the H_2 desorption trace displays peaks at $T_{max} \approx 300$ and 342 K. The peak at 342 K is not well resolved in some of the data and appears as a tail which extends to ~400 K. The qualitative aspects of the H_2 and CO desorption data are largely invariant with coverage. For example, the CO desorption temperature maximum shifts only 13 K, from 423 to 410 K, as the exposure to $HCOOCH_3$ is increased from 0.6 to 4.8 L (L = langmuir). The width of the peak, however, almost doubles as the exposure is increased above 1.2 L. These results are consistent with the desorption behavior of low coverages of CO on Ni(111) as measured in our laboratory and as reported in the literature.[16,17] A very weak CO_2 peak, <2% of the CO desorption intensity, was observed in the region of 320–400 K for each of the three molecules.

Desorption of methane and acetaldehyde was observed during the decomposition of ethyl formate on Ni(111). The acetaldehyde peak (m/e = 29) appears at 327 K and the methane peak at 274 K. This result is in a general sense similar to what is observed for ethanol decomposition on clean Ni(111). Gates *et al.*[18] have shown that the latter process leads to desorption of acetaldehyde and methane at close to 280 K. However, our observation is peculiar in the sense that the methane desorption is complete before the onset of acetaldehyde desorption. According to Gates *et al.*,[18] the decomposition of ethoxy on Ni(111) also deposits a small concentration of carbon on the surface. This was not checked for in our experiments. Desorption of neither CH_4, C_2H_4, nor C_2H_6 was observed for methyl acetate on Ni(111).

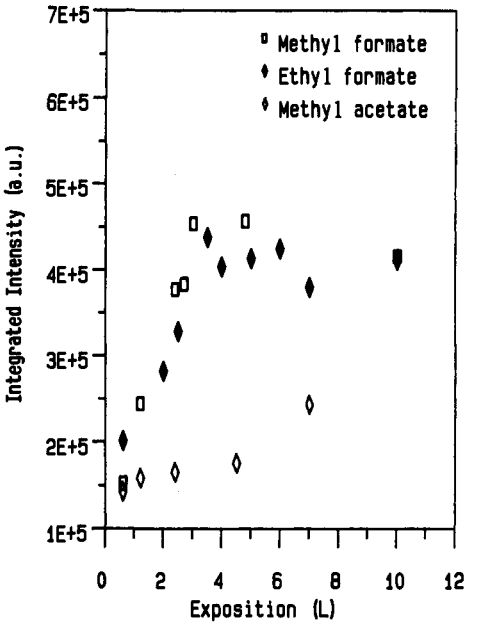

Figure 5. Integrated CO desorption intensity as a function of exposure to MF, EF, and MA at 86 K. The CO desorption peak is observed at ~410 K.

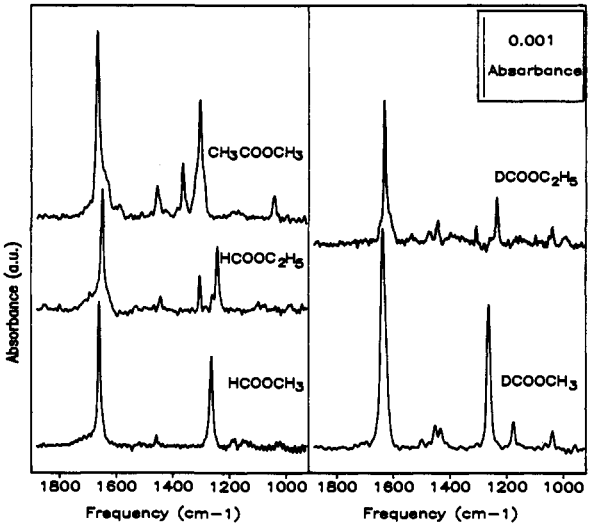

Figure 6. RAIRS spectra for submonolayer coverages of methyl formate (MF), ethyl formate (EF), and methyl acetate on Ni(111) at 86 K. Spectra for methyl formate and ethyl formate deuterated on the carbonyl carbon are included.

Two important differences emerge on comparing the TPD data for methyl acetate with those for the two formate molecules. First, as may be seen from Figures 2–5, the molecular desorption peak from the chemisorbed layer occurs at a higher temperature for methyl acetate than for the other two molecules. Second, the amount of CO which desorbs as a result of the decomposition of methyl acetate is much less than that for the formate molecules. The latter information is shown in Figure 5. This figure also indicates that dissociation of methyl acetate only occurs for low exposures (~1 L), whereas dissociation of methyl formate and ethyl formate continues to exposures of ~4 L. The dosing conditions for each of the three molecules was kept the same for the experiments presented in Figure 5.

2. RAIRS Results. Simple esters display relatively simple infrared spectra.[19] However, the interpretation of the spectra is complicated by substantial coupling among several of the normal modes of vibration.[20-23] Typically, the CH_3, CHO, and COC

(15) Zahidi, E.; Castonguay, M.; McBreen, P. H. To be submitted for publication.
(16) Surnev, L.; Xu, Z.; Yates, J. T., Jr. *Surf. Sci.*, **1988**, *201*, 1.
(17) Zhang, R.; Gellman, A. J. *Langmuir* **1993**, *9*, 449.
(18) Gates, S. M.; Russell, J. N., Jr.; Yates, J. T., Jr. *Surf. Sci.* **1984**, *146*, 199.

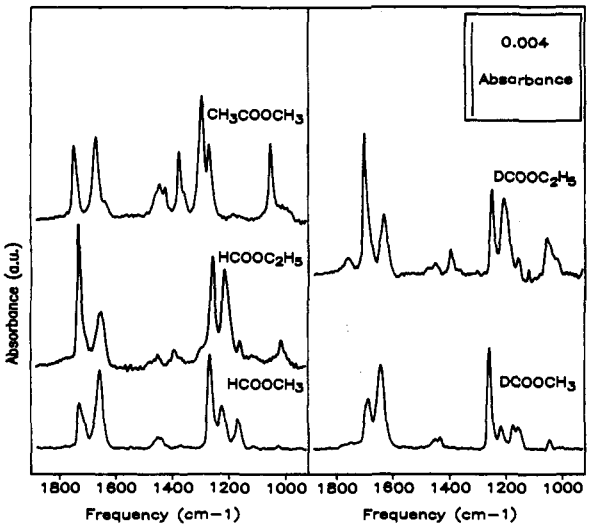

Figure 7. RAIRS spectra for more than monolayer coverage of methyl formate, ethyl formate, and methyl acetate on Ni(111) at 86 K.

Table 1. Vibrational Frequencies for Adsorbed, Condensed, and Matrix-Isolated Methyl Formate (MF)

MF ads		MF	Cu-	Cu/	MF	mode and symmetry	approximate[20]
$\theta \rightarrow 0$	$\theta \rightarrow 1$	cond	(110)[2]	SiO_2[7]	gas[20]	species	description
	3042		3050		3033	(ν_1, a′)	CH_3 a.s.
					3014	(ν_{13}, a″)	CH_3 a.s.
	2985		2980		2963	(ν_2, a′)	CH_3 s.s.
					2938	(ν_3, a′)	CH s.
				1722			
1659	1659	1730	1670	1665	1746	(ν_4, a′)	C═O s.
1458	1460		1450		1459	(ν_5, a′)	CH_3 a.b.
					1446	(ν_{14}, a″)	CH_3 a.b.
	1442				1434	(ν_6, a′)	CH_3 s.b.
					1372	(ν_7, a′)	CH b.
1262	1262	1220	1260		1205	(ν_8, a′)	C_1–O_e s.; CH_3 r.; C–O_e s.
	1182		1180		1162	(ν_9, a′)	CH_3 r.; OCO b.; C_1–O_e s.; C–O_e s.
					1158	(ν_{15}, a″)	CH_3 r.
					1044	(ν_{16}, a″)	CH o.p.w.
		916	920		921	(ν_{10}, a′)	C–O_e s.; C_1–O_e s.
				720	767	(ν_{11}, a′)	OCO b.
					338	(ν_{17}, a″)	COC t.
			370		308	(ν_{12}, a′)	COC b.
					130	(ν_{18}, a″)	CH_3 t.

groups are directly coupled to each other.[23] An overview of the RAIRS spectra obtained for submonolayer and condensed layer exposures is given in Figures 6 and 7, respectively. Figure 6 displays peaks characteristic of the chemisorbed layer, whereas Figure 7 displays peaks arising from both the chemisorbed layer and the condensed layer. A tabulation of the observed RAIRS frequencies as well as published assignments for the modes of the free molecules is given in Tables 1–3. An assignment of some of the intense RAIRS peaks will be discussed in the next section. However, simply by comparison to the characteristic strong infrared absorption bands of esters,[19–26] we can make a preliminary assignment of the intense features at ~1650 and ~1260 cm^{-1} to the ν(C═O) (carbonyl) and $\nu(C_1–O_e)$ stretching vibrations, respectively. For greater than monolayer exposures, Figure 7, a carbonyl stretching frequency characteristic of the condensed layer appears at a higher frequency. In contrast, the $\nu(C_1–O_e)$ mode is at lower frequency in the condensed layers than in the chemisorbed layers. The chemisorption-induced shifts which we

Table 2. Vibrational Frequencies for Adsorbed, Condensed, and Solution Ethyl Formate (EF)

EF/Ni(111)		EF/	EF/	mode and	approximate
$\theta \rightarrow 0$	$\theta \rightarrow 1$	Ni(111) cond	CCl_4[19]	symmetry	description[19]
			2985	(ν_{18}, a″)	CH_3 a.s.
	2974		2968	(ν_{19}, a″)	CH_2 a.s.
	2942		2938	(ν_1, a′)	CH_3 a.s.
			2928	(ν_2, a′)	CH s.
			2912	(ν_3, a′)	CH_2 s.s.
			2876	(ν_4, a′)	CH_3 s.s.
1650	1650	1732	1732	(ν_5, a′)	C═O s.
		1474	1475	(ν_6, a′)	CH_2 b.
		1460	1467	(ν_7, a′)	CH_3 a.b.
1444	1444		1443	(ν_{20}, a″)	CH_3 a.b.
			1385	(ν_8, a′)	O═C–H b.
	1394		1373	(ν_9, a′)	CH_3 s.b.
			1362	(ν_{10}, a′)	CH_2 w.
1304			1300	(ν_{21}, a″)	CH_2 t.w.
1242	1255	1215	1187	(ν_{11}, a′)	C–O–C a.s.; (C_1–O_e) s.
	1160		1152	(ν_{12}, a′)	CH_3 r.
			1108, 1097	(ν_{22}, a″)	CH_3 r.
	1013		1007	(ν_{13}, a′)	C–C s.
			920	(ν_{23}, a″)	O═C–H o.p.b.
			842	(ν_{24}, a″)	CH_2 r.
			810, 750	(ν_{14}, a′)	C–O–C s.s.
			672	(ν_{15}, a′)	O═C–O b.
			384, 448	(ν_{16}, a′)	O–C–C b.
			325	(ν_{17}, a′)	C–O–C b.
			244, 268	(ν_{25}, a″)	C–O t.
			170	(ν_{26}, a″)	C–CH_3 t.
			60, 80	(ν_{27}, a″)	O–CH_2 t.

Table 3. Vibrational Frequencies for Adsorbed, Condensed, and Gas-Phase Methyl Acetate (MA)

MA ads	MA cond	MA gas[24]	mode and symmetry	approximate description[24]
		3028	(ν_1, a′)	(O)CH_3, a.s.
		3028	(ν_2, a′)	(C)CH_3 a.s.
		3002	(ν_{18}, a″)	(O)CH_3 a.s.
		3002	(ν_{19}, a″)	(C)CH_3 a.s.
		2955	(ν_3, a′)	(O)CH_3 s.s.
		2940	(ν_4, a′)	(C)CH_3 s.s.
1666	1749	1747	(ν_5, a′)	C═O s.
		1462	(ν_{20}, a″)	(O)CH_3 a.b.
1456		1455	(ν_6, a′)	(O)CH_3 a.b.
		1445	(ν_{21}, a″)	(C)CH_3 a.b.
	1442	1438	(ν_7, a′)	(C)CH_3 a.b.
	1423	1438	(ν_8, a′)	(O)CH_3 s.b.
1364		1372	(ν_9, a′)	(C)CH_3 s.b.
1302	1266	1249	(ν_{10}, a′)	(C_1–O_e) s.
		1190	(ν_{11}, a′)	(O)CH_3 r.
		1161	(ν_{22}, a″)	(O)CH_3 r.
1041		1051	(ν_{12}, a′)	O–CH_3 s.
			(ν_{23}, a″)	(C)CH_3 r.
		982	(ν_{13}, a′)	(C)CH_3 r.
		846	(ν_{14}, a′)	C–O_e s.
		638	(ν_{15}, a′)	C═O i.b.
		609	(ν_{24}, a″)	C═O o.b.
		433	(ν_{16}, a′)	O–C–C b.
		302	(ν_{17}, a′)	C–O–C b.
		203	(ν_{25}, a″)	C–O t.
			(ν_{26}, a″)	O–C t.
			(ν_{27}, a″)	C–C t.

(19) Charles, S. W.; Jones, G. I. L.; Owen, N. L.; Cyvin, S. J.; Cyvin, B. N, *J. Mol. Struct.* **1973**, *16*, 225.
(20) Muller, R. P.; Hollenstein, H.; Huber, J. R., *J. Mol. Spectrosc.* **1983**, *100*, 95.
(21) Hollenstein, H.; Gunthard, Hs. H., *J. Mol. Spectrosc.* **1980**, *84*, 457.
(22) Susi, H.; Scherer, J. R. *Spectrochim. Acta* **1969**, *25A*, 1243.
(23) Susi, H.; Zell, T. *Spectrochim. Acta* **1933**, *19*, 1963.
(24) Dybal, J.; Krimm, S. *J. Mol. Struct.* **1988**, *189*, 383.
(25) Wilmshurst, J. K. *J. Mol. Spectrosc.* **1957**, *1*, 204.
(26) George, W. O.; Houston, T. E.; Harris, W. C. *Spectrochim. Acta* **1974**, *30A*, 1035.

Table 4. Shifts in the ν(C=O) and ν(C–O_e) Modes of Esters Caused by Adsorption and by Complexation with Lewis Acids

	methyl formate						ethyl formate				methyl acetate			
mode	gas	adsorbed on Ni(111)	adsorbed on Cu(110)	adduct BF_3	adduct BCl_3	adsorbed on Cu/SiO_2	soln CCl_4	adsorbed on Ni(111)	adduct $TiCl_4$	adduct $FeCl_3$	gas	adsorbed on Ni(111)	adduct BF_3	adduct BCl_3
ν(C=O)	1746	1659	1670	1653 1635	1618	1666	1732	1653	1635	1630	1747	1666	1619	1560
ν(C–O_e)	1205	1262	1260	1348	1337		1187	1255	1260	1305	1249	1302	1360	1370

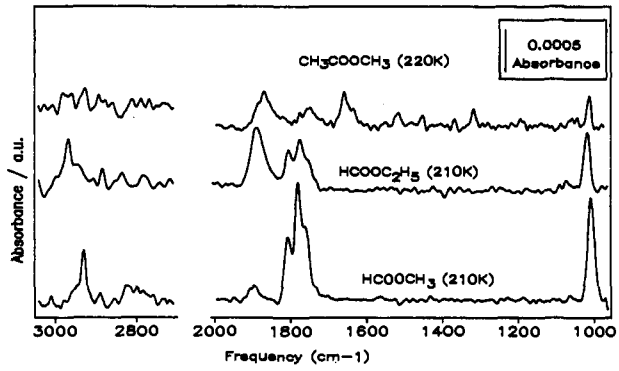

Figure 8. RAIRS spectra recorded on annealing the MF, EF, and MA exposed surfaces to above 200 K. The initial exposure, at 86 K, was 7 L in each case.

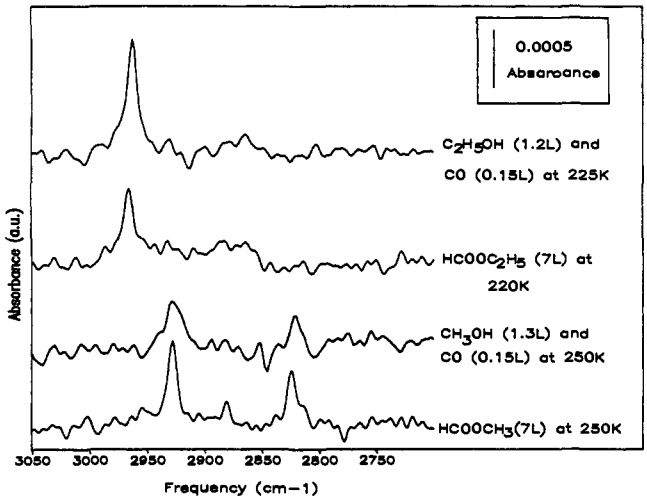

Figure 9. More detailed spectra in the CH stretching region for the samples annealed to above 200 K. Data are also included for CO coadsorbed with ethoxy and methoxy species.

observe for the ν(C=O) and ν(C–O_e) vibrations of MF, EF, and MA on Ni(111) may be estimated from the data listed in Table 4. Literature data are also included in Table 4, for ester–Lewis acid addition compounds[27–29] and for methyl formate adsorbed on copper.[1,7,11]

The CH stretching region of our spectra is not very informative, especially in the submonolayer regime. The data were obtained using a narrow-band MCT detector and additional work using an InSb detector is required. Note, however, that the weak CH stretching signal is to a large part intrinsic to the adsorption system. We know this because, as shown below (Figures 8–10), a satisfactory ν(CH) signal is obtained for the adsorbed decomposition products methoxy and ethoxy. Furthermore, coadsorption of NO with the esters leads to a significant increase in the ν(CH) signal, presumably through either a change in the order of the surface layer or a change in the molecular orientation.

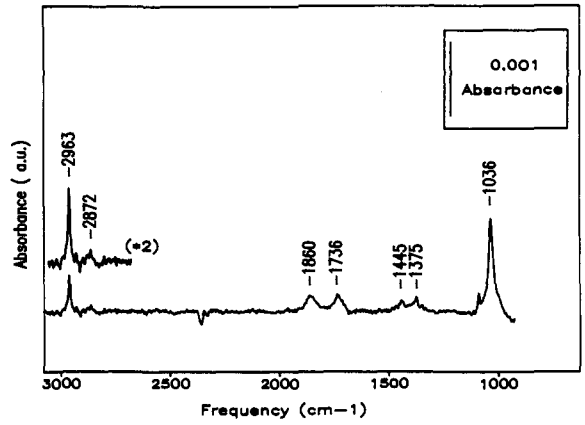

Figure 10. A complete RAIRS spectrum for the coadsorption of CO and ethoxy. The coadsorbed system was prepared by warming an ethanol (1.2 L) and CO (0.15 L) exposed surface to 225 K.

These coadsorption experiments are underway and will be published separately. For the purposes of this paper we will concentrate on the 2100–900-cm^{-1} region of the spectra of the adsorbed esters.

An overview of the RAIRS spectra of surface species formed by annealing the adsorption systems to above 200 K, subsequent to exposure to 0.6 L at 86 K, is shown in Figure 8. Additional data for anneal temperatures less than 200 K are below in Figure 14. Complete removal of the RAIRS features characteristic of adsorbed methyl formate and ethyl formate is observed for the spectra recorded at 210 K. The RAIRS features characteristic of chemisorbed methyl acetate are, however, not completely removed at 220 K. Annealing to 210 K replaces the methyl formate spectrum with one characteristic of coadsorbed methoxy and carbon monoxide. Similarly, the spectrum of ethyl formate is replaced by one characteristic of coadsorbed ethoxy and CO. Adsorbed alkoxy and methoxy species typically produce an intense ν(CO) stretching feature at ~1040 cm^{-1},[31] as observed in Figure 8. The disappearance, or decomposition, of the adsorbed esters may be monitored by observing the intensities of the ν(C=O) and ν(C–O_e) bands at ~1650 and ~1260 cm^{-1}, respectively. The co-adsorbed CO which is produced in each case displays a complex spectrum consisting of several peaks in the range 1700–1900 cm^{-1}. These CO_{ads} spectra will be discussed in detail elsewhere.[35] The annealed methyl acetate system consists of a mixture of features assigned below to methyl acetate, acetyl (CH_3-CO), methoxy, and CO. Additional data on the CH stretching region of the alkoxy spectra are displayed in Figure 9. The latter spectra display more clearly resolved features and are interesting for comparison with RAIRS spectra of adsorbed methoxy and ethoxy on otherwise clean metals. A list of the observed frequencies for methoxy and ethoxy prepared by the surface decomposition of the ester molecules is given in Table 5. It can be seen that there is exceptionally good agreement between our values and those obtained by others through decomposition of methanol[32,33] and ethanol[34] on clean Ni(111). In a series of calibration experiments, we coadsorbed CO and methanol as well

(27) Dembitskŭ, A. D.; Sumarokova, T. N. *Opt. Spectrosc.* **1962**, *12*, 202.
(28) Paul, R. C.; Chandha, S. L.; Vashisht, J. L. *Indian J. Chem.* **1969**, *7*, 276.
(29) Taillandier, M.; Liguier, J.; Taillandier, E. *J. Mol. Struct.* **1968**, *2*, 437.
(30) Zahidi, E.; Castonguay, M.; McBreen, P. H. In preparation.
(31) Dai, Q.; Gellman, A. J. *Surf. Sci.* **1991**, *257*, 103.
(32) Demuth, J. E.; Ibach, H. *Chem. Phys. Lett.* **1979**, *60*, 395.
(33) Zenobi, R.; Xu, J.; Yates J. T., Jr.: Persson, B. N. J.; Volokitin, A. I. *Chem. Phys. Lett.* **1993**, *208*, 414.

Table 5. Vibrational Frequencies (cm^{-1}) for Adsorbed Methoxy and Ethoxy Species on Ni(111)

adsorbed methoxy from					adsorbed ethoxy from		
methyl formate		methyl acetate			ethyl formate		
7 L	0.6 L	7 L	0.6 L	methanol[a]	7 L	0.6 L	ethanol[a]
2928	2928	2927		2927	2965	2967	2963
2880				2881	2883	2883'	2872
2824	2825			2817	1445		1445
1434					1377		1375
1014	1009	1012	1019	1018 (1759)[a]	1024	1019	1036 (1736)[a]

[a] These experiments involved formation of the alkoxy species from the parent alcohol in the presence of the coadsorbed CO. The stretching frequency of the coadsorbed CO is given in parentheses.

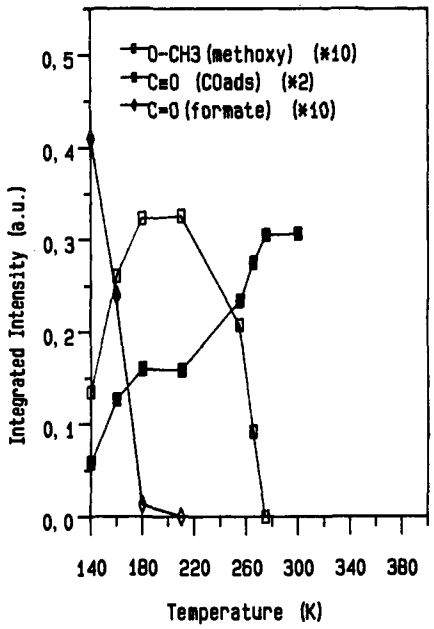

Figure 11. Plots of integrated absorbances for RAIRS peaks characteristic of adsorbed methyl formate, adsorbed methoxy, and adsorbed CO. The carbonyl stretching vibration (ν_4) is used for methyl formate and the ν(C–O) vibration for methoxy. The CO signal is the sum over all the observed CO peaks.

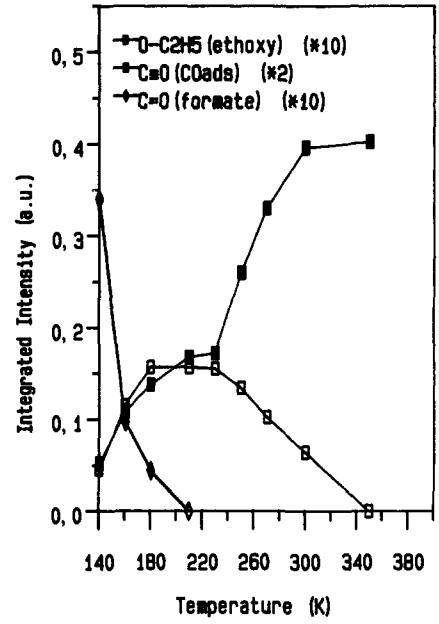

Figure 12. Plots of integrated absorbances for RAIRS peaks characteristic of ethyl formate, ethoxy, and CO on Ni(111). The carbonyl stretching mode (ν_5) was used for EF, the ν(C–O) mode for ethoxy, and all the observed ν(CO) peaks for CO.

as CO and ethanol on Ni(111). The observed frequencies taken from these experiments are also listed in Table 5. The main point to note is that adsorbed CO in the presence of methoxy yields a ν(CO) peak at 1759 cm^{-1}. Similarly, CO coadsorbed with ethoxy produces a peak at 1736 cm^{-1}. The value of 1736 cm^{-1} corresponds quite well with the low-frequency vibrational envelope seen at ~1726 and 1735 cm^{-1}, respectively, in the spectra of MF and EF shown in Figure 8. A RAIRS spectrum of coadsorbed CO and ethoxy is shown in Figure 10.

Spectacular changes in the distribution of the adsorbed carbon monoxide signal occur on heating to higher temperatures. These results are complex and will be presented in detail separately.[35] However, a semiquantitive idea of the overall changes which occur on annealing may be taken from Figures 11–13. These figures show how the integrated absorbances of bands characteristic of the adsorbed ester, and the CO and alkoxy surface products, vary as a function of anneal temperature. They also serve to summarize several of the main points of this paper. Decomposition of methyl formate and ethyl formate begins at approximately 140 K and leads to coincident growth of the CO_{ads} and alkoxy signals. This first stage of the decomposition is complete at approximately 190 K and the methoxy and ethoxy species remain stable to approximately 220 K. Then, as the temperature is increased further, the alkoxy species dissociate providing a new source of adsorbed CO. Decomposition of the alkoxy species is complete at 300 K for methoxy and 350 K for ethoxy, and the CO signal remains stable to above 350 K. As shown in Figures 2–4, CO desorption occurs at ~410 K. Note, however, that methyl acetate (Figure 13) produces a somewhat different behavior. The main difference is that the initial decomposition begins at a higher temperature, ~180 K as compared to ~140 K for methyl and ethyl formate. As a result the subsequent step, wherein the methoxy species dissociates, begins before the first step is complete for all the monolayer. For methyl acetate, there is then no plateau region where the methoxy is stable on the surface, as is the case for methyl formate and ethyl formate. We show, in the following section, that there is evidence for the formation of a stable acetyl species in the decomposition of methyl acetate on Ni(111). The spectra displayed in Figure 14 show that both MF and EF undergo some dissociation at 140 K whereas MA is intact at 175 K.

Discussion

The discussion will be divided into three sections: the molecular orientation of the adsorbed esters, their decomposition pathways, and a comparison of the surface chemistry of the three molecules.

1. Molecular Orientation. Methyl formate has the simplest infrared spectrum, consisting of twelve in-plane (a') and six out-of-plane (a'') vibrations, and will be discussed first. Following the work of Muller et al.,[20] a listing of the observed frequencies for argon matrix isolated methyl formate is given in Table 1. The approximate description of the vibrational modes, as given by the

(34) Xu, J. X.; Zhang, R.; Zenobi, J.; Yoshinobu, Xu; Yates, J. T., Jr. *Surf. Sci.* **1991**, *256*, 288.
(35) Zahidi, E.; Castonguay, M.; McBreen, P. H. To be submitted for publication.

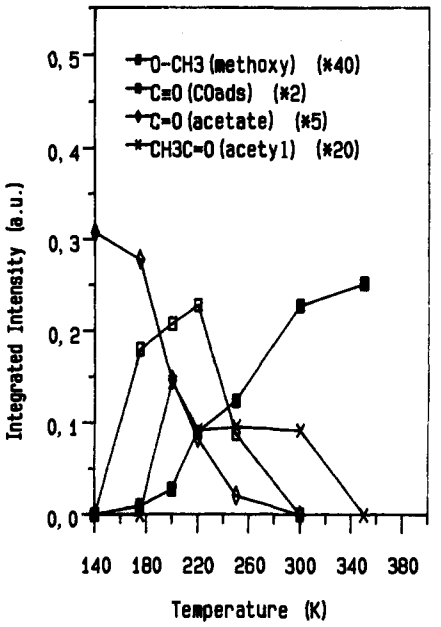

Figure 13. Plots of integrated absorbances for RAIRS peaks characteristic of methyl acetate, methoxy adsorbed acetyl, and CO. The carbonyl stretching mode (ν_5) was used for methyl acetate. A feature at 1518 cm^{-1} is assigned to the CO stretching vibration of adsorbed acetyl.

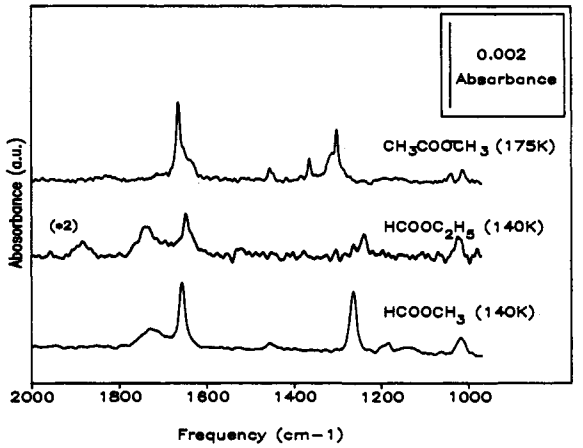

Figure 14. RAIRS data obtained on annealing the MF and EF exposed surfaces to 140 K and a MA exposed surface to 175 K.

latter authors, is also included. The RAIRS spectrum of methyl formate chemisorbed on Ni(111), Figure 6, resembles that of the isolated molecule in the sense that the intense and characteristic ν_4 and ν_8 modes are observed. However, there are important differences in that the latter modes are shifted as indicated in Table 4. There is also an important difference between the HREELS spectrum of methyl formate on Cu(110) and the RAIRS spectra for Ni(111). The ν_{10} mode is absent in the RAIRS spectra whereas it gives rise to an intense feature at 920 cm^{-1} in the HREELS spectrum of methyl formate on Cu(110).[1,2] We will assign the observed modes, and comment on the missing ones, in the context of the orientation of MF on Ni(111). A description of the general features of the chemisorption bond to the surface is implicit in a description of the molecular orientation on the surface.

In considering the adsorption geometry we can assume that adsorbed methyl formate retains the molecular plane which makes it belong to the C_s point group. This is because the available data on the conformational analysis of methyl formate show that the gauche conformation is unstable by ~50 kJ mol^{-1} relative to the cis and trans isomers.[3,36] The cis isomer is ~19 kJ mol^{-1} more stable than the trans isomer by virtue of the attractive interaction between the C=O and O$_e$–C dipoles.[3,37,38] We can then determine whether or not the molecular plane is oriented parallel to the surface. For the parallel orientation only the a″ modes should be active, whereas for perpendicular adsorption only the a′ modes would have dynamic dipole moment components normal to the surface. The submonolayer spectra display absorption bands corresponding to the ν_4 (1659 cm^{-1}) and ν_8 (1262 cm^{-1}) modes, each of which are a′. These same modes appear at 1730 and 1220 cm^{-1}, respectively, in the RAIRS spectrum of the condensed layer, Figure 7. The assignments and observed shifts are consistent with the analysis of the HREELS spectrum of MF on Cu(110)[1,2] and IR and Raman spectra of ester–Lewis acid adducts,[27,29] as listed in Table 4.

Free methyl formate (Table 1) displays three features in the $\delta(CH_3)$ region and hence we cannot unambiguously assign the observed feature at 1458 cm^{-1}. However, its frequency is closest to that of the ν_5 mode, an asymmetric deformation, which also belongs to the totally symmetric representation. The $DCOOCH_3$ spectra display a feature at 1040 cm^{-1} which may be assigned to the in-plane D–CO bending vibration.[20] By combining the $HCOOCH_3$ and $DCOOCH_3$ data, we observe three (or possibly four) modes in the 2000–900 cm^{-1} region, all of which are a′. This enables us to rule out the case in which the molecular plane is parallel to the surface. The question then arises as to why the ν_{10} mode is not observed in the RAIRS spectra despite the fact that it is an a′ mode and that it yields an intense peak at 920 cm^{-1} in the HREELS spectrum of MF on Cu(110) and a relatively strong feature in the spectrum of free methyl formate. One explanation for these discrepancies is that the ν_{10} mode is attenuated by the strict surface selection rule operative in RAIRS measurements of adsorbates on metal surfaces. On the basis of the work of Muller *et al.*,[20] the potential energy distribution of the ν_{10} mode of $HCOOCH_3$ may be written as ν_s(O–CH_3) [81] + ν_s(HCO–O) [14]. If we assume that the same description applies to the adsorbed molecule, we can estimate the RAIRS activity of the ν_{10} mode for the adsorption geometry shown below. For this geometry, the ν_{10} mode should be attenuated since the principal motion involves stretching the O–CH_3 bond which is roughly parallel to the surface.

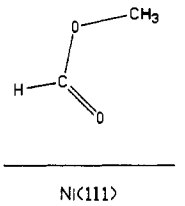

Likewise, ν_6, the symmetric $\delta_s(CH_3)$ mode, would be attenuated. This is consistent with our assignment of the peak at 1458 cm^{-1} to the asymmetric ν_5 mode. The ν_{10} mode is detected at 916 cm^{-1} in the condensed layer spectrum, where it produces a relatively weak peak. Note that our signal-to-noise ratio degrades severely below ~920 cm^{-1} and this may be a contributing factor in attenuating the ν_{10} peak. In addition, based on data for the interaction of methyl formate with BF_3,[29] it is possible that a strong donor interaction between the carbonyl lone pair and the nickel surface could red shift the ν_{10} vibration by as much as 25 cm^{-1}. This would render its detection even more difficult.

The RAIRS spectrum of ethyl formate on Ni(111) displays a striking coverage dependence.[15] Some bands grow in with increasing coverage and others fade out. A detailed rationalization of these variations is presented elsewhere.[15] Here we concentrate on the low coverage spectrum. Three intense features are observed in the 2000–900-cm^{-1} region. By analogy to the solution (CCl_4)

(36) Nagy, P.; Kiss, A. I.; Lopata, A. *J. Mol. Struct.* **1981**, *86*, 41.

(37) Blom, C. E.; Gunthard, Hs. H. *Chem. Phys. Lett.* **1981**, *84*, 267.

(38) Rushkin, S.; Bauer, S. H. *J. Phys. Chem.* **1980**, *84*, 3061.

phase spectrum[19] and the spectra of ethyl formate–Lewis acid adducts,[27,28] the peaks are assigned as follows: ν_5 (1650 cm^{-1}), ν_{21} (1304 cm^{-1}), and ν_{11} (1242 cm^{-1}). The ν_5 vibration is the carbonyl stretch mode, ν_{21} is a CH_2 twisting mode, and ν_{11} is principally the HCO–O stretching vibration. If the assignment of the feature at 1304 cm^{-1} is correct, then at least some of the adsorbate must be present in the syn-gauche conformation. This conformer form is present at the level of 59% at room temperature in gas phase ethyl formate.[19] The CH_3 groups project out at 95° from the OCO plane in the syn-gauche conformer.[39] In the syn-trans configuration, the molecule displays C_s symmetry and the out-of-plane twisting vibration, ν_{21}, would be RAIRS inactive. Both the ν_5 and ν_{11} modes are intense at all coverages, however the latter mode shifts to higher frequency as the coverage is increased. The rather significant changes which occur in other regions of the spectrum are interpreted elsewhere in terms of adsorption-induced isomerization[15] which occurs as monolayer coverage is approached. The general similarity of the RAIRS spectra of adsorbed ethyl formate with those for methyl formate suggests that the same orientation and bonding configuration holds in both cases. That is, adsorption occurs via the carbonyl lone pair with the result that the molecule is oriented approximately perpendicular to the surface.

Methyl acetate adsorbed on Ni(111) displays five well resolved relatively intense peaks in the 2000–800-cm^{-1} region. With reference to the gas phase spectrum,[24] four of the peaks may be assigned as follows: ν_5 (1666 cm^{-1}), ν_9 (1364 cm^{-1}), ν_{10} (1302 cm^{-1}), and ν_{12} (1041 cm^{-1}). The remaining intense feature appears in the $\delta(CH_3)$ region and cannot be unambiguously assigned. As in the case for MF and EF, the assigned modes all belong to the a′ representation, indicating that the molecular plane of adsorbed MA is also perpendicular to the surface. The shifts in the carbonyl (ν_5), C_1–O_e (ν_{10}), and O–CH_3 (ν_{12}) stretching frequencies are all in the same sense as that for methyl acetate complexed to BCl_3 or BF_3.[29] As in the case of MF and EF, these shifts indicate that MA chemisorbs on the Ni(111) surface through the interaction of a carbonyl lone pair.

The above analysis, based on symmetry considerations, may be viewed from a more chemical perspective. As discussed in more detail by Walczak *et al.*,[40] an oxygenate such as methyl formate is expected to bond to the surface via either the ester oxygen or the carbonyl group. The HOMO orbital of methyl formate is the carbonyl oxygen lone pair (n_O) and the second highest occupied molecular orbital (SHOMO) is the conjugation modified lone pair orbital (p_1) which is mainly localized on the ester oxygen.[41] The LUMO orbital is the π^* carbonyl orbital, which is both empty and sufficiently low in energy to participate in back-bonding.[40] However, back-bonding will be efficient only in the η^2 configuration wherein the carbonyl group is roughly parallel to the surface. The intense ν_4 band which we observe at 1660 cm^{-1} is not consistent with the η^2 configuration, but it is consistent with a η^1 configuration where the C=O bond axis has a vector component normal to the surface. Steric considerations, in addition to the fact that the HOMO orbital is the carbonyl lone pair, probably account for the fact that chemisorption occurs solely via the carbonyl group. The molecular desorption temperatures are also consistent with the proposed mode of adsorption.[42] That is, the desorption temperature from the monolayer is close to that expected for the interaction of one oxygen lone pair with the surface. Additional interaction of the ester oxygen with the surface would lead to a significantly higher desorption energy.[42] Of course, the TPD data only give information on the mode of chemisorption of the fraction of molecules which desorb molecularly. Therefore, the bulk of evidence for the interaction via the carbonyl group rests on the RAIRS data.

2. Thermal Chemistry of Esters on Ni(111). The combined RAIRS and TPD measurements lead to an unambiguous description of the stable surface and gas-phase products of the thermal decomposition of the three ester molecules on Ni(111). Two plausible decomposition pathways are available to an ester on a metal surface. In one pathway the C_1–O_e bond could be broken to form an adsorbed alkoxy species. In the second, the O_e–R_2 bond could be broken to produce a formate species on the surface.

$$R_1COOR_2 \rightarrow R_{1,ads} + CO_{ads} + OR_{2,ads} \quad (1)$$

$$R_1COOR_2 \rightarrow R_1COO_{ads} + R_{2,ads} \quad (2)$$

Reaction 2 would lead to the desorption of CO_2 whereas reaction 1 would yield CO as the desorption product. Formate decomposition on Ni(111) yields substantial CO_2 desorption.[43] The TPD results, Figures 2–4, show desorption of CO but not of CO_2. This indicates selective cleavage of the C_1–O_e bond, as in reaction 1, for each of the three molecules studied. TPD is an indirect method of determining the surface chemistry as it measures only the final volatile decomposition products. Furthermore, some of these products may arise from recombination reactions on the surface. RAIRS, on the other hand, can probe the adsorbed intermediates in the decomposition process. This application of RAIRS is extremely straightforward in the present case since the various possible adsorbed oxygenate intermediates display highly characteristic IR spectra. This is a consequence of the high symmetry of the species involved and the large dynamic dipole associated with the carbon–oxygen bonds. The RAIRS spectra presented in Figure 8, which were obtained by annealing to around 230 K, display features which may be clearly attributed to adsorbed methoxy in the case of methyl formate and methyl acetate and adsorbed ethoxy in the case of ethyl formate. These conclusions are based on data taken from the literature[32-34] and our calibration spectra, Figures 9 and 10, for methanol and ethanol decomposition on Ni(111). A complete listing of the observed vibrational frequencies is given in Table 5. The data show no evidence, however, for ν(OCO) modes characteristic of adsorbate formate species.[44] Hence, we can unambiguously rule out reaction 2 in favor of reaction 1. As discussed below, the decomposition of methyl acetate results in the formation of a stable R_1CO_{ads} (acetyl) species.

The infrared spectra of the alkoxy species on metal surfaces is interesting per se. For example, the assignment of the vibrational modes in RAIRS spectra of adsorbed methoxy is still an open question.[45,48] A related problem is a determination of the orientation of the methoxy species with respect to the surface.[46] The spectrum which we observe for methoxy derived from methyl formate on Ni(111) is very similar to the spectrum for methoxy on clean Ni(111) reported by Zenobi *et al.*[33] The latter authors report vibrational bands at 1027, 2817, 2878, and 2921 cm^{-1}. Following the work of Dastoor *et al.*[47] and Jayasooriya *et al.*,[48] we assign the bands at 2928 and 2824 cm^{-1} to the ν_{as}(CH) and ν_s(CH) stretching modes of a tilted methoxy species. We observe an additional feature in the methyl deformation region at 1434 cm^{-1} for high initial coverages of methyl formate. The RAIRS spectrum which we observe for ethoxy derived from ethyl formate

(39) Riveros, J. M.; Wilson, E. B., Jr. *J. Chem. Phys.* **1967**, *46*, 4605.
(40) Walczak, M. M.; Leavitt, P. K.; Thiel, P. A. *J. Am. Chem. Soc.* **1987**, *109*, 5621.
(41) Sweigert, D. A.; Turner, D. W. *J. Am. Chem. Soc.* **1972**, *94*, 5592.
(42) Sexton, G. A.; Hughes, A. E. *Surf. Sci.* **1984**, *140*, 227.
(43) Erley, W.; Sander, D. *J. Vac. Sci. Technol.* **1989**, *A7*, 2238.
(44) Weisel, M. D.; Chen, J. G.; Hoffman, F. M.; Sun, Y.-K.; Weinberg, W. H. *J. Chem. Phys.* **1992**, *97*, 9396.
(45) Chesters, M. A.; Cash, E. M. *Spectrochim. Acta* **1987**, *43A*, 1625.
(46) Linder, Th.; Somers, I.; Bradshaw, A. M.; Kilcoyne, A. L. D.; Woodruff, D. P. *Surf. Sci.* **1988**, *208*, 333.
(47) Dastoor, H. E.; Gardner, P.; King, D. A. *Chem. Phys. Lett.* **1993**, *209*, 493.
(48) Jayasooriya, U. A.; Anson, C. E.; Al-Jowder, O.; D'Alfonso, G.; Stanghellini, P. L.; Rossetti, R. *Surf. Sci.* **1993**, *294*, 131.

is also very similar to the RAIRS spectrum reported by Xu *et al.*[34] for ethoxy on clean Ni(111). They assigned bands at 2964 and 2875 cm^{-1} to $\nu_{as}(CH_3)$ and $\nu_s(CH_2)$ modes, respectively. The excellent agreement, in terms of both the relative intensities and the positions of the peaks, of our results with those obtained by Yates' group[34] clearly indicate that decomposition of methyl formate and ethyl formate is exclusively via reaction 1. The situation for methyl acetate is a bit more complex, although it is also basically consistent with reaction 1. First, the concentration of surface species produced by methyl acetate decomposition is smaller (Figures 5 and 8) than is the case for the other two molecules. Hence the features in the RAIRS spectra are correspondingly weaker. Second, the RAIRS spectra obtained at 220 K (Figure 8) display a feature at 1517 cm^{-1} in addition to features which may be attributed to coadsorbed CH_3COOCH_3, CO, and methoxy by reference to the spectra for $HCOOCH_3$ decomposition (Figure 8) and the spectrum of chemisorbed methyl acetate (Figure 6). This additional feature shifts to 1528 cm^{-1} at 300 K, a temperature at which CH_3COOCH_3 and methoxy are completely removed from the surface. In the context of methyl acetate decomposition, a band at 1517–1528 cm^{-1} is immediately suggestive of an adsorbed acetyl (CH_3CO) intermediate. Davis and Barteau[49] found that acetyl produced on Pd(111) via acetaldehyde decomposition yielded a ν(CO) feature at 1565 cm^{-1}. Furthermore, they found that the acetyl intermediate decomposed over the 250–350 K temperature range. In our case, we note from Figure 13 that the intensity of the 1517-cm^{-1} feature is maximized at 200 K, that it decreases between 200 and 220 K, and that it subsequently remains constant until removal occurs between 300 and 350 K. Hence, the stability of the acetyl intermediate on Ni(111) is reasonably consistent with that on Pd(111).

The surface decomposition of R_1COOR_2 molecules, such as those under study, may be considered as a chemical method for the preparation of adsorbed states of CO.[35] The distribution of the ν(CO) intensity among the different states is a complicated function of temperature and initial coverage of the ester molecules.[35] In this paper, we will concentrate on the total integrated intensity of the peaks due to adsorbed carbon monoxide and on the low-frequency peaks which appear coincidently with the formation of the alkoxy species. As shown in Figure 14, annealing the methyl formate and ethyl formate exposed surfaces to 140 K results in the emergence of broad peaks centered at 1726 and 1735 cm^{-1}, respectively. These frequencies are rather low for CO adsorbed on annealed Ni(111). Furthermore, there is a possibility that adsorbed formyl species contribute to these low-frequency peaks. For example, η_1-HCO on Ru(001) displays a carbonyl stretching mode at 1730 cm^{-1}.[50] If the features which we observe are indeed due to HCO_{ads}, then they indicate that the surface decomposition proceeds via C_1–O_e bond cleavage followed by CH bond scission in an unstable HCO_{ads} intermediate. However, another explanation exists for the low-frequency ν-(CO) features in our spectra, namely the influence of coadsorbed alkoxy on the CO vibrational frequency. Species, such as methoxy, which induce strong work function changes are well-known to strongly perturb the internal stretching frequency of coadsorbed CO. For example, Richter and Ho[51] used HREELS to monitor the transformation of methanol on Ni(110) to coadsorbed CO and methoxy. The lowest ν(CO) frequency which they detected was 1810 cm^{-1} at 180 K. Similarly, Dastoor *et al.*[47] report that CO perturbed by the presence of adsorbed methoxy on Ni(110) displays an adsorption band at 1808 cm^{-1}. However, in our systems, the adsorbed CO is formed simultaneously with the alkoxy species at ≥140 K, rather than through the decomposition of the alkoxy species or through background adsorption prior to the experiment. In light of this difference, we performed calibration experiments by preparing methoxy and ethoxy species from the parent alcohols in the presence of CO. The parent alcohols were adsorbed at 86 K, annealed to 110 K, and subsequently exposed to CO at 86 K. Methoxy and ethoxy were prepared under these conditions by annealing the surface to 225 and 250 K, respectively. The results shown in Figure 10 and Table 5 display a low-frequency ν(CO) feature at 1736 cm^{-1}. These results, then indicate that the low-frequency ν(CO) feature observed at 140 K in our spectra (Figure 14) is due to adsorbed CO rather than HCO_{ads}. This is consistent with the observation by Richter and Ho[52] that H_2CO decomposes on Ni(110) at 95 K but does not produce a HCO_{ads} intermediate stable enough for detection in their HREELS experiments. We are setting up for time-resolved RAIRS measurements in order to search for kinetic isotope effects in the decomposition of $HCOOR_2$ and $DCOOR_2$ on Ni(111). These experiments are required to conclusively decide whether or not a HCO_{ads} species is involved in the decomposition sequence.

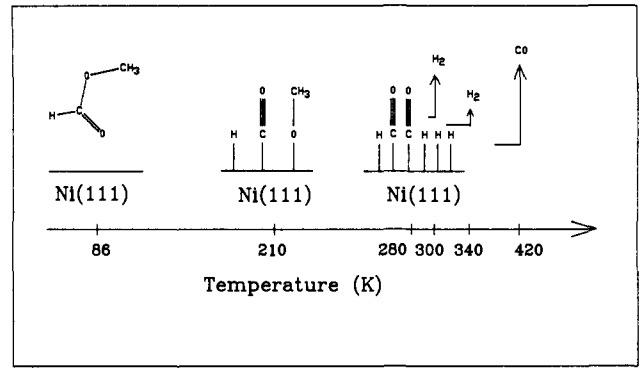

Figure 15. A schematic illustration of the decomposition process for methyl formate on Ni(111).

3. Comparison of the Surface Chemistry of Methyl Formate, Ethyl Formate and Methyl Acetate on Ni(111). The overall surface chemistry which we observe for the ester molecules on Ni(111) is simpler than that observed in thermolysis studies of these molecules. Ethyl formate thermolysis leads to HCOOH and C_2H_4.[53,54] Methyl formate pyrolysis produces CH_3OH, CO, CH_4, CO_2, and H_2CO.[37] Methyl acetate pyrolysis produces methyl radicals and CO_2[55,56] as well as CH_3OH, CH_2CO, CH_4, H_2CO, and possibly C_2H_6.[37] The decomposition of each of these three esters on Ni(111) occurs via C–O_e bond cleavage, as in reaction 1, leading to adsorbed CO and alkoxy species. The decomposition process for methyl formate is schematically illustrated in Figure 15.

Data on the formation and decomposition of the surface species are shown in Figures 12–14. These figures display the evolution of the integrated absorbance of a characteristic band of the parent molecule, CO_{ads}, and the alkoxy species as a function of anneal temperature. Although the integrated absorbances need not necessarily be a linear function of surface concentration, the plots clearly demarcate the various steps in the decomposition process. The decomposition of methyl formate and ethyl formate to H_{ads}, CO_{ads}, and $OR_{2\,ads}$ begins at ≥140 K, consistent with an identical rate determining step in both cases. Methyl acetate, on the other hand, begins to decompose at temperatures ≥175 K. Methoxy decomposition sets in at ≥220 K and is complete at ~280 K. Ethoxy decomposition begins at ≥240 K and is complete at ~320 K. These observations are in reasonably good agreement with

(49) Davis, J. L.; Barteau, M. A. *J. Am. Chem. Soc.* **1989**, *111*, 1782.
(50) Mitchell, W. J.; Wang, Y.; Xie, J.; Weinberg, W. H. *J. Am. Chem. Soc.* **1993**, *115*, 4381.
(51) Richter, L. J.; Ho, W. *J. Chem. Phys.* **1985**, *83*, 2569.
(52) Richter, L. J.; Ho, W. *J. Chem. Phys.* **1985**, *83*, 2165.
(53) Blades, A. T.; Sandhu, H. S. *Int. J. Chem. Kinet.* **1971**, *3*, 187.
(54) Pereira, R. C. L.; Isolani, P. C. *J. Phtotochem. and Photobiol. A.* **1988**, *42*, 51.
(55) ulzmann, K. G. P.; Baxter, D. E.; Khazra, M.; Lund, T. S. *J. Phys. Chem.* **1985**, *89*, 3561.
(56) Hintsa, E. J.; Wodtke, A. M.; Lee, Y. T. *J. Phys. Chem.* **1988**, *92*, 5379.

what is known about the decomposition of ethanol and methanol on Ni(111).[57-59] Gates *et al.* found that ethoxy decomposition on Ni(111) occurs at ≥260 K[57] and methoxy decomposition at ≥240 K.[58]

Note, from Table 4, that the adsorption induced shifts in the ν(C=O) and $\nu(C_1-O_e)$ modes are approximately equal for the three molecules. This indicates that the adsorption induced modifications of the internal bonds are roughly similar in each case. This is to be expected since adsorption occurs through the carbonyl lone pair in each case. However, the decomposition temperature for methyl acetate is ~35 K higher than that for the other two molecules. Furthermore, the observation of an acetyl species, in addition to CO_{ads} and $OCH_{3\ ads}$, indicates that C_1-O_e and CC bond cleavage are competitive processes for methyl acetate on Ni(111). The interaction of the carbonyl lone pair of methyl acetate with the metal will result in a strengthening of the CC bond,[29] making it more difficult to break. On the other hand, the H–CO bond in ethyl formate and methyl formate will be weakened by the trans effect of the carbonyl lone pair .[60] The fact that the activation energy for methyl acetate dissociation is relatively high results in decomposition slightly above the temperature at which it begins to desorb from Ni(111). The contrary holds for methyl formate and ethyl formate. A consequence of this difference is that desorption is quite competitive with decomposition in the case of methyl acetate. As a result, the TPD and RAIRS data, Figures 5 and 8, respectively, show that methyl acetate forms a smaller amount of surface products than either of the other two molecules.

The RAIRS data indicate that each of the esters is bound to the surface via the carbonyl oxygen. The interaction of the oxygen lone pair orbital with the metal accounts for the red shift in the carbonyl stretching frequency. Recall, for example, that the ν_4 mode of methyl formate is shifted down by 71 cm^{-1} (Table 1) from the condensed phase value. Sexton *et al.*[1,2] observed a shift of 50 cm^{-1} for methyl formate on Cu(110). The larger shift observed for methyl formate on Ni(111) is consistent with the fact that nickel is a better electron acceptor than copper. A summary of some of the reasons why this is so is given elsewhere.[61] The shifts, downward for the carbonyl mode and upward for the R_1CO-O mode, shown in Table 4, are almost as large as those reported by Paul *et al.*[28] and Dembitskii and Sumarokova[27] for addition compounds of esters with Lewis acids such as tin tetrachloride. Even larger shifts, in the same directions, are observed for the interaction of esters with very strong acceptor molecules such as BCl_3 and BF_3.[29] The weak charge transfer complex, methyl acetate–iodine,[62] displays shifts of ~20 cm^{-1} which is less than what we observe. The consequences of the implied electron donation interaction, in terms of the internal bonds of the esters, have been discussed by several authors.[27,29,63] They point out that the bond order of the carbonyl bond is reduced. Similarly the bond order of the R_1CO-O bond is increased due to conjugation with the alkoxy oxygen lone pair. The fact that the RAIRS data indicate that the ester–Ni(111) chemisorption bonding is similar to ester–Lewis acid interactions is of potential significance. The origin of this significance lies in the use of Lewis acids to induce stereoselective attack of carbonyl carbon in molecules such as esters.[64,65] This point is discussed elsewhere[15] in the context of RAIRS evidence for adsorption induced isomerization of esters on Ni(111).

Conclusion

We have used RAIRS and TPD to study the chemisorption of methyl formate, ethyl formate, and methyl acetate on Ni(111). The major results of the study may be summarized as follows:

(i) Adsorption of all three molecules occurs through the interaction of a carbonyl lone pair orbital with the surface. This interaction leads to shifts in the vibrational spectrum similar to those measured for ester–Lewis acid addition compounds.

(ii) The adsorbed molecules are oriented with their molecular planes roughly perpendicular to the surface. Only vibrational modes belonging to the a′ representation were detected.

(iii) The desorption products, in each case, were CO and H_2. Desorption of acetaldehyde and methane also occurred from ethyl formate on Ni(111).

(iv) Decomposition occurred at ≥140 K for methyl formate and ethyl formate but at ≥175 K for methyl formate. We speculate that H–CO bond breaking is the rate determining step in the decomposition of methyl formate and ethyl formate. In the case of methyl acetate we observed an acetyl (CH_3CO_{ads}) decomposition product.

(v) Heating of a coadsorbed CO/ethanol layer produces a carbon monoxide stretching band shifted down to 1736 cm^{-1}.

Acknowledgment. Partial funding for this research has been provided by the Networks of Centers of Excellence in Molecular and Interfacial Dynamics. Funding for the project was also made available through an NSERC research grant. M.C. acknowledges an NSERC scholarship for graduate studies. We acknowledge the contribution of A. Bouffard to the machining of the experimental system.

(57) Gates, S. M.; Russell, J. N. Jr., Yates, J. T., Jr. *Surf. Sci.* **1986**, *171*, 111.
(58) Gates, S. M.; Russell, J. N. Jr., Yates, J. T., Jr. *Surf. Sci.* **1985**, *159*, 233.
(59) Zhang, R.; Gellman, A. J. *Catal. Lett.* **1993**, *17*, 47.
(60) Fang, H. L.; Meister, D. M.; Swofford, R. L. *J. Phys. Chem.*, **1984**, *88*, 410.
(61) McBreen, P. H.; Roy, J. R.; Serghini Monim, S. Submitted for publication.
(62) Yamada, H.; Kozima, K. *J. Am. Chem. Soc.* **1960**, *82*, 1543.
(63) Meaune, M. T.; Odiot, S. *J. Mol. Struct.* **1972**, *11*, 147.
(64) Shambayatti, S.; Crowe, W. D.; Schreiber, S. L. *Angew. Chem., Int. Ed. Engl.* **1990**, *29*, 256.
(65) Corey, E. J.; Loh, T.-P.; Sashar, S.; Azimiorara, M. *Tetrahedron Lett.* **1992**, *33*, 6945.